CrossMark

Dissociation of polar oil components in low salinity water and its impact on crude oil–brine interfacial interactions and physical properties

Rasoul Mokhtari[1] · Shahab Ayatollahi[2]

Abstract

Despite many efforts into the study of fluids interaction in low salinity water flooding, they are not probing the basics of transport phenomena between the involved phases. This work is aimed to bring new understanding of fluid–fluid interaction during low salinity water flooding through a series of organized experiments in which a crude oil sample with known properties was kept in contact with different brine solutions of various ionic strengths. Measuring brine pH, conductivity and crude oil viscosity and density for a period of 45 days illustrates the strong effect of the contact time and ionic strength on the dissociation of polar components and physical properties of the crude oil and brine. Besides, the interfacial tension (IFT) measurements show that the interfacial interactions are affected by several competitive interfacial processes. By decreasing the ionic strength of the brine, the solubility of naphthenic acids in the aqueous solution increases, and hence, the conductivity and the pH of the aqueous phase decrease. To verify this important finding, UV–Vis spectroscopy and ^{1}H NMR analysis were also performed on aged brine samples. Notably, there is an ionic strength of brine in which the lowest IFT is observed, while the other physical properties are remained relatively unchanged.

Keywords Ionic strength · Oil–brine interaction · Physical properties · Contact time · Polar components

1 Introduction

Water flooding as a secondary oil recovery method has been one of the most common and efficient fluid injection methods over a century. This can be attributed to various reasons, including high water availability that leads to lower capital and operating costs and high efficiency in displacing light to medium API oils. Therefore, water flooding is technically and economically preferred compared to other enhanced oil recovery techniques (Austad 2013; Kazemi Nia Korrani 2014; Mohanty and Chandrasekhar 2013; Yousef et al. 2010). Recently, much research has shown that controlling the composition and salinity of the injected water (known as low salinity water) disturbs the equilibrium condition and, hence, results in higher oil recovery efficiency through favorable influence on oil/brine/rock interactions compared to common seawater flooding (Al-Attar et al. 2013; Al-Shalabi and Sepehrnoori 2016; Austad 2013; Austad et al. 2011; Emadi and Sohrabi 2013; Gupta and Mohanty 2011; Karimi et al. 2016; Li 2011; Morrow and Buckley 2011; Nasralla et al. 2011; RezaeiDoust et al. 2009; Seccombe et al. 2008; Strand et al. 2006; Tang and Morrow 1997, 1999; Yildiz and Morrow 1996; Zaeri et al. 2018). Among various mechanisms suggested for low salinity water, the complex crude oil/aqueous solution interactions are not yet well understood. Several studies have been undertaken to investigate the sensitivity of interfacial properties of the brine–oil interface to the salinity and ions of the aqueous phase (Cai et al. 1996; Guo et al. 2013; Hiemenz and Rajagopalan 1997; Lashkarbolooki et al. 2014a, 2016a, c; Serrano-Saldaña et al. 2004; Yarranton and Masliyah 1996; Yousef et al. 2010). The provided results are different, even contradictory with ambiguous explanations.

✉ Shahab Ayatollahi
   dr.ayatollahi@gmail.com; shahab@sharif.ir

[1] School of Chemical and Petroleum Engineering, Shiraz University, Shiraz, Iran

[2] Sharif Upstream Petroleum Research Institute (SUPRI), Chemical and Petroleum Engineering Department, Sharif University of Technology, Tehran, Iran

Resins and asphaltene molecules also play an important role in determining the interfacial interactions of brine–crude oil (Abdel-Wali 1996; Cratin 1993; Lashkarbolooki et al. 2014b, 2016b; Lashkarbolooki and Ayatollahi 2016). Abdel-Wali studied the impact of simple polar components on crude oil (including both simple acid and base materials such as naphthenic acids (R-COOH) and basic nitrogen-containing components such as octadecylamine (R-NH$_2$)) by adding various concentrations of oleic acid and octadecylamine (ODA) to crude oil, and also they investigated the effect of salinity of the brine, through altering the concentration of NaCl in the brine in the range of 0–200,000 ppm. They encountered a reverse trend for IFT by adding salts and oleic acids and reported specific salinity and concentration of oleic acid and octadecylamine at which the minimum interfacial tension is achieved. They believed that the increase in IFT by increasing salinity above the optimum point is related to the attachment of Na$^+$ ions to the hydrophilic part of the oil sample, which reduces the solubility of oleic acids in the water phase, but they didn't mention the reasons behind the IFT reduction in the salinity below the optimum salinity point (Abdel-Wali 1996). Polar components are the simple acid and base materials which exist in crude oil and act as surface active materials. The polar components stem from the heteroatoms present in the heavier fractions (Seifert and Howells 1969; Speight 2014). Compounds that contain oxygen are most commonly alcohols, phenols, carboxylic acids, ketones, esters and ethers. These are often acidic in nature, and the collective term naphthenic acid (NA) is often used in reference to them. Common basic nitrogen-containing compounds are pyridine and quinolone, and non-basic compounds are typically pyrrole, indole and carbazole and their derivatives. Sulfur compounds commonly found in crude oils are thioalkanes and heterocyclic compounds derived from thiophene (Schobert 2013).

As a novel insight and in order to investigate the effect of brine salinity on interfacial interactions, Moradi et al. studied the role of ionic strength on dissociation of crude oil's naphthenic acids (NAs) in water through NMR spectroscopy for a 7-day period. The results showed that the concentration of NAs dissolved in the aqueous phase increases as the salinity of brine, which is in contact with crude oil, decreases (Moradi et al. 2013). However, they did not clarify the effect of this dissolution on the other physical properties of crude oil and brine. Although NAs are weak acids and do not disassociate entirely in aqueous solution, even this limited dissociation may affect the physical properties of brine and govern its interfacial behavior. Although there are some research works trying to identify the role of polar components on the interfacial performance between crude oil and brine and their effects on IFT and emulsion stability (Alvarado et al. 2011;

Czarnecki et al. 2013; Garcia-Olvera et al. 2016; Mohammed and Sorbie 2009, 2010), the mechanisms involved and the effect of contact time on the physical properties of reservoir fluids are ambiguous. Therefore, this work is aimed to design a series of organized experiments to assess the interactions between brine and crude oil in contact for a period of 45 days. In addition to the flow behavior of the fluids through the porous media, any changes in physical properties of reservoir fluids such as crude oil density and viscosity as well as brine pH and conductivity may control the release of the trapped residual oil. In this study, an Iranian crude oil sample with known properties was selected and then kept in contact with brines of different salinities. Brine pH and conductivity as well as crude oil viscosity and density were measured at specific time intervals during the contact time of 45 days. Also, photographs were captured from interfaces to show the changes during this period for different brines. Besides, a set of IFT measurement tests were designed which will be discussed in detail in the following sections. Moreover, in order to accurately verify the results and identify the mechanisms, a set of ultraviolet–visible (UV–Vis) and one-dimensional nuclear magnetic resonance (^{1}H NMR) spectroscopy analysis were also utilized.

2 Materials and methods

In order to investigate the changes in fluid properties by time, 200 mL of aqueous phase was poured into the preserving and sampling setup, as is shown in Fig. 1. Then
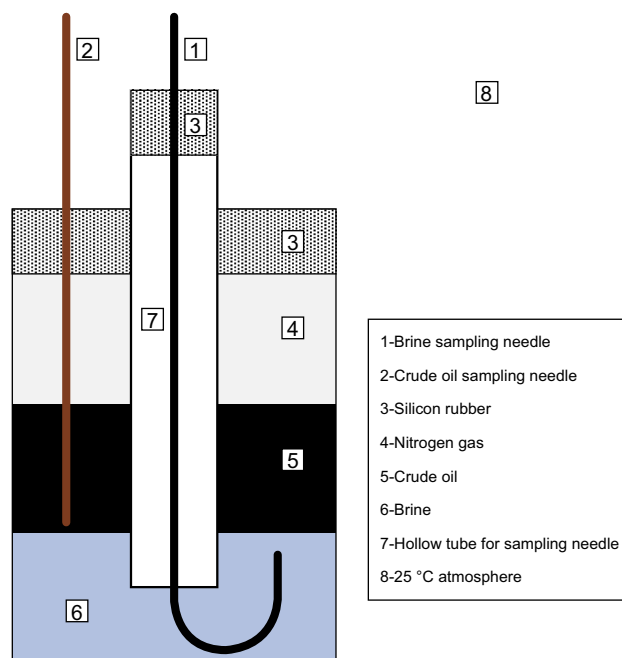

1-Brine sampling needle
2-Crude oil sampling needle
3-Silicon rubber
4-Nitrogen gas
5-Crude oil
6-Brine
7-Hollow tube for sampling needle
8-25 °C atmosphere

Fig. 1 Schematic diagram of preserving and sampling setup

250 mL of crude oil was gradually added, and it was gently maintained at laboratory temperature of 25 °C. To exclude the effect of emulsification due to shear and simulate the critically low flow rate of imbibed water into matrix in fractured reservoirs, the mixtures were not shaken during the test period. During core aging for inspecting rock–fluid interactions (such as Amott cell procedure) usually about 1000-h period is considered as a standard test duration (McPhee et al. 2015). Hence, this standard test duration (45 days) was considered for fluid–fluid interaction experiments in this study. The samples at specific times of 0, 10, 20, 30 and 45 days after preparation were taken from each phases to evaluate the specific properties. Samples were gently collected from a distance near to the interface of the brine–crude oil using a fixed specific type of sampler which allowed us to take brine samples from the same position with respect to the brine–oil interface. Brine and crude oil which stay in contact with each other for a period of time are called aged brine and aged crude oil, respectively.

Different measurements such as pH and conductivity tests were taken on the aged water samples, while the viscosity and density tests were conducted on the aged crude oil samples. Also three different categories of IFT tests were designed as follows: (1) fresh brine–aged crude oil, (2) aged brine–fresh crude oil and (3) aged brine–aged crude oil, to clarify the main mechanisms. In addition, a set of UV–Vis and ^{1}H NMR spectroscopy were performed on aged brines after 45 days.

2.1 Crude oil specification

Crude oil sample originating from a southwest Iranian oil field, labeled KL, was used in this study. It was analyzed in order to determine the asphaltene content and total acid number (TAN). The asphaltene content and TAN of the crude oil were measured according to ASTM-D6560-12 and ASTM-D664 standard procedures, respectively. The properties of the used crude oil are shown in Table 1. Also Table 2 represents the composition of KL crude oil.

2.2 Brine composition

All brine samples were prepared in the laboratory and filtered through a 0.43-μm Millipore filter and evacuated to remove the dissolved air. The formation water (FW) was

from the same southwest Iranian oil reservoir. In addition, the seawater (SW) was prepared to have the ionic strength of 0.832 mol/L, the same as Persian Gulf seawater. The initial SW was then diluted by adding deionized water to obtain solutions with 2 and 10 times diluted SW. The notations "2-TDSW" and "10-TDSW" stand for 2 and 10 times diluted seawater with ionic strength of 0.416 and 0.0832 mol/L, respectively, as they are listed in Table 3.

2.3 pH and conductivity measurements

The pH and conductivity of all brine samples were measured at 25 °C, using a Bench-Top Meter Model 860032 manufactured by Sper Scientific. The apparatus was calibrated for pH and conductivity prior to any measurement using standard buffers and KCl solutions with known values of pH and conductivity. All experiments were done at least in triplicate, and the mean values are reported here.

2.4 UV–Vis spectroscopy

UV–Vis absorbance was measured in 1-cm path length quartz cells by a spectrophotometer (Model T80, PG Instruments, UK). The UV–Vis spectra of aged brine samples were recorded at 25 °C in absorption mode in the wavelength range of 190–400 nm, compared with fresh brine as the reference.

2.5 NMR spectroscopy

Mixtures of 90% H_2O–10% D_2O were made by mixing 540 μL of the aged water with 60 μL of D_2O. NMR spectroscopy measurements were taken on the prepared samples at 400 MHz on a Bruker Avance III Ultrashield 400 instrument. In order to estimate the chemical shifts, H_2O was determined as the standard reference. All experiments were accomplished with a width of 16 ppm at 25 °C. Solvent suppression into the calibrated pulse sequence of 11.5 s 90° was used. In order to eliminate the effect of conductivity changes, the experimental results were controlled and corrected with PABA calibrated standards to enable the comparison between brines of different electrical conductivities. Because of the low solubility of the NAs in the aqueous phase, these ^{1}H NMR spectroscopy experiments were specially performed to precisely quantify the dissolved organic components in the brine.

Table 1 Physical properties of crude oil

Crude oil name	Total acid number, mg KOH/g oil	Asphaltene content, wt%	Density at 25 °C, g/cm^3	Viscosity at 25 °C, cP
KL	0.14	0.6	0.84	7.5

Table 2 Composition of crude oil

Composition, mol%											Molecular weight of crude oil	Molecular weight of C_{7+}	Specific gravity of C_{7+}
H_2S	CO_2	C_1	C_2	C_3	$i\text{-}C_4$	$n\text{-}C_4$	$i\text{-}C_5$	$n\text{-}C_5$	C_6	C_{7+}			
2.33	2.58	47.59	8.83	5.09	0.94	2.43	1.02	1.22	1.67	26.26	195	209.7	0.8634

Table 3 Prepared brine composition

	Composition, ppm							Total dissolved solids, ppm	Ionic strength, mol/L
	NaCl	KCl	$MgCl_2$	$CaCl_2$	Na_2SO_4	$NaHCO_3$	$CaCO_3$		
FW	140,314	0	2854	40,286	2586	2014	1628	189,682	3.674
SW	28,424	825	6430	1384	4490	106	0	41,659	0.832
2-TDSW	14,200	400	3215	690	2244	84	0	20,833	0.416
10-TDSW	2842	82	642	138	448	10	0	4162	0.0832

2.6 Viscosity measurement

Viscosity of the crude oil samples at different contact times was measured using a Cannon–Fenske capillary viscometer calibrated at 25 °C. The measurements for each sample were taken in triplicate, and the average value was reported as the crude oil sample viscosity.

2.7 Density measurement

Density of the crude oil samples was measured using an Anton Paar DMA^{TM} 35 density meter for different contact times at 25 °C. This apparatus measures the density of the samples with an accuracy of 0.001 g/mL in a few seconds and utilizes only two milliliters of sample. Each test was the average of three measurements, and value was considered to be the density of the sample.

2.8 IFT measurement

The accurate measurement of the interfacial tension between crude oil and brine is essential to investigate the interface interactions. The changes in IFT values and the trend of these changes can lead to valuable insights into the phenomena taking place at the interface. The most recently used method of IFT measurement is the pendant drop (Drelich et al. 2002; Peters and Arabali 2013). A schematic of utilized experimental apparatus is given in Fig. 2. This apparatus (DSA 100, KRUSS, Germany) consists of a view cell, a syringe pump and an image capturing and processing system.

2.9 Visual study

Since samples from the interface are utilized to qualitatively and quantitatively determine the interface conditions and the effect of salinity on the interfacial behavior, it is important to have consistent sampling. For this purpose all samples were gently collected from the same position in crude oil and close to the interface. Each sample was then photographed using a Dino AM-351 digital microscope with adjustable magnification up to 600×. The image processing toolbox of MATLAB programming software was used to measure the size distribution, mean size and volume fraction of water droplets and asphaltene agglomerates.

3 Results and discussion

3.1 pH and conductivity measurement

To assess any crude oil–brine interaction phenomenon, brine pH and conductivity were measured at specific times during the period of 45 days and the crude oil and the brine were in contact with each other. The results are shown in Figs. 3 and 4.

Figure 3 illustrates critical pH changes for 10-TDSW, where it was reduced from its initial value of 7.45 to 4.8. The pH of the FW, SW and 2-TDSW exhibited almost no significant changes during the test period. The reason may be the partitioning of the crude oil polar components and natural surfactants such as asphaltenes and naphthenic acids.
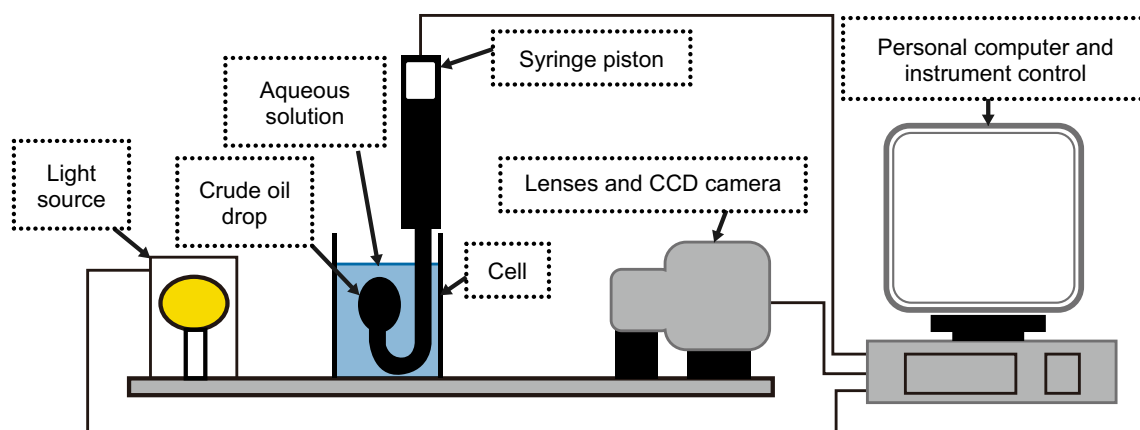
Fig. 2 Schematic view of interfacial tension measurement apparatus. (Lashkarbolooki and Ayatollahi 2016)
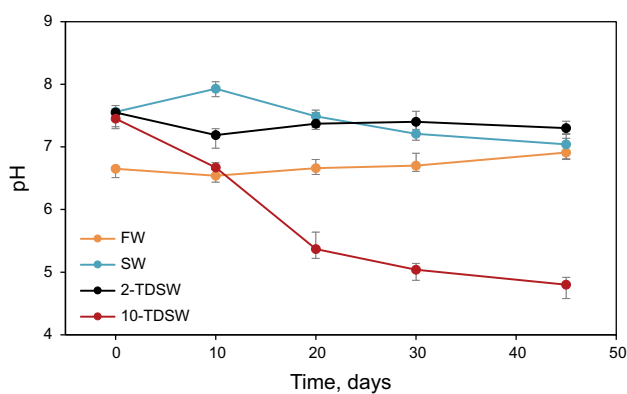

Fig. 3 pH of the brines in contact with the crude oil during 45 days
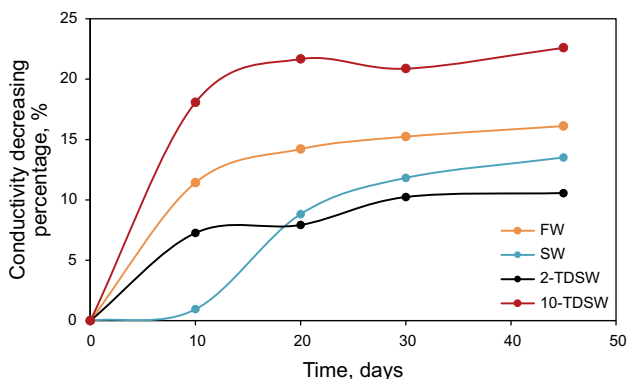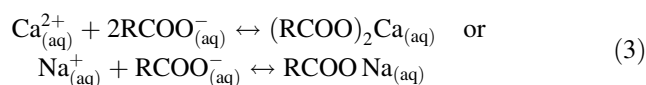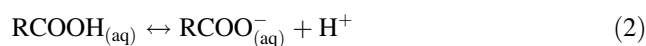

Fig. 4 Conductivity decrease for various brine solutions during 45 days of being in contact with crude oil

Since NAs are hydrophilic, they tend to adsorb at the crude oil–brine interface and dissociate in water. The partitioning phenomenon of NAs through equilibrium reactions is explained here (Moradi et al. 2013):

$$RCOOH_{(o)} \leftrightarrow RCOOH_{(aq)} \qquad (1)$$

$$RCOOH_{(aq)} \leftrightarrow RCOO^-_{(aq)} + H^+ \qquad (2)$$

$$Ca^{2+}_{(aq)} + 2RCOO^-_{(aq)} \leftrightarrow (RCOO)_2Ca_{(aq)} \quad \text{or}$$
$$Na^+_{(aq)} + RCOO^-_{(aq)} \leftrightarrow RCOO\,Na_{(aq)} \qquad (3)$$

According to reaction 1, naphthenic acids enter the brine phase where they dissociate and produce carboxylic anions and hydrogen ions (reaction 2). Obviously, the release of hydrogen ions in the aqueous phase results in a pH reduction. As a result of the salting-in effect, at lower salinities, more NAs partition and dissociate in the aqueous phase. According to the aforementioned hypothesis, Fig. 3 indicates that the more effective the partitioning is, subsequently, the lower the pH values. Figure 4 also depicts the conductivity decrease for various brine solutions, which confirms the dissociation of some nonconductive organic impurities into the aqueous phase. Obviously, 10-TDSW has the maximum conductivity decrease rate, as well as its rate of pH change. These changes may affect other brine–crude oil properties such as IFT, which will be explained in more detail later.

3.2 UV–Vis spectroscopy

In order to verify the previous conclusions and suggested mechanisms based on partitioning of NAs from the crude oil into the brines, UV–Vis spectroscopy was performed. For this purpose, the aged brines were examined after 45 days of being in contact with crude oil. To ensure that any spectral adsorption is solely due to the NAs partitioned into brine and also to exclude the effect of salinity, the apparatus was calibrated with fresh brine of the same salinity prior to each test. Figure 5 shows the absorption spectra for different brines. According to the Beer–Lambert law, absorption and concentration of NAs in the solutions are directly proportional. Therefore, as is depicted in
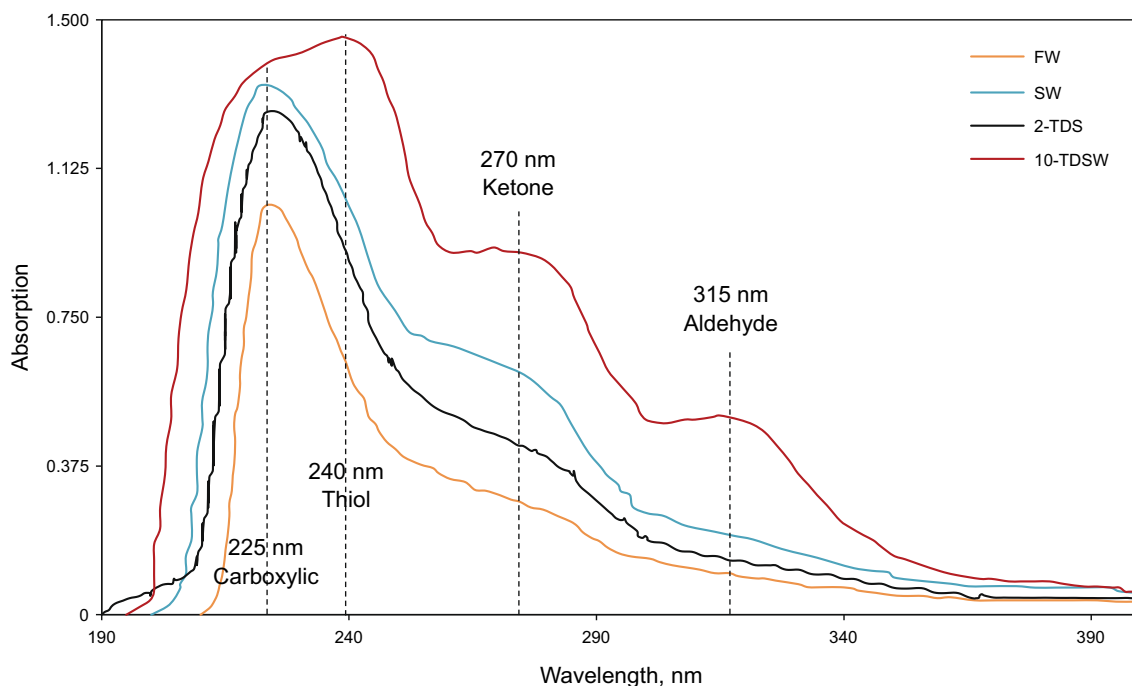
Fig. 5 Absorption spectra of different brines after 45 days of being in contact with crude oil

Fig. 5, 10 SW and FW have the highest and lowest concentration of NAs, respectively.

The UV spectroscopy results are consistent with the pH and conductivity experiments. High concentration of NAs in 10-TDSW is the sole reason for a significant reduction in pH value. It is worth mentioning that the concentration of NAs in 2-TDSW is much less than in 10-TDSW and SW. This may not because of a lower dissociation potential of 2-TDSW; rather it may due to the high polarization of the interface for this salinity. This hypothesis is investigated through IFT measurements in the following sections.

3.3 ^{1}H NMR spectroscopy

The major characteristic peaks in NMR spectra in Fig. 6 indicate the presence of naphthenic acids including thiol, ketone and aldehyde in 0–2 ppm range (Badertscher et al. 2009; Moradi et al. 2013). Hence, to accurately compare the differences between various brine solutions, the results are represented in 0–2 ppm range in Fig. 6.

In addition, the whole range of 10-TDSW NMR spectrum was also added to the top-left corner of Fig. 6 which indicates the presence of the carboxylic functional group at 2.1 ppm. In agreement with the data from UV–Vis spectroscopy, 10-TDSW shows higher peak intensity than other brines, which indicates the presence of higher amounts of NAs in this brine. As depicted in Fig. 6, the intensities of the signals in the spectra collected from the 2-TDSW brine are lower than SW and 10-TDSW solutions. In general, this

reveals that the concentration of NAs increases as the brine salinity decreases. This conclusion has an exception at 2-TDSW in which some of NAs may transfer from the bulk toward the interface and accumulate there. This phenomenon may have significant effects on interfacial interactions.

3.4 Viscosity and density measurement

In addition to the previous assessment of the partitioning phenomenon, any changes in the fluid composition and physical properties can be traced through viscosity and density measurements of crude oil in contact with the brines of different salinities. Figure 7 shows the obtained viscosity trends for the aged oil in contact with different aqueous phases.

Since all parameters affecting the viscosity such as temperature, sampling and experimental procedure were the same, the variation in viscosity is attributed to the aging of the oil in the vicinity of the aqueous phase. The dissolution of polar components in water, especially when two phases are in a static condition, is diffusion controlled and is accelerated when the salinity of the brine is reduced (Hamam et al. 1988). On the other hand, the naturally existing polar components in crude oil such as naphthenic acids, resins and asphaltenes are adsorbed on the interface, which can produce water-in-oil emulsions. Several studies have been accomplished to investigate the effect of different parameters such as temperature, pressure, polar
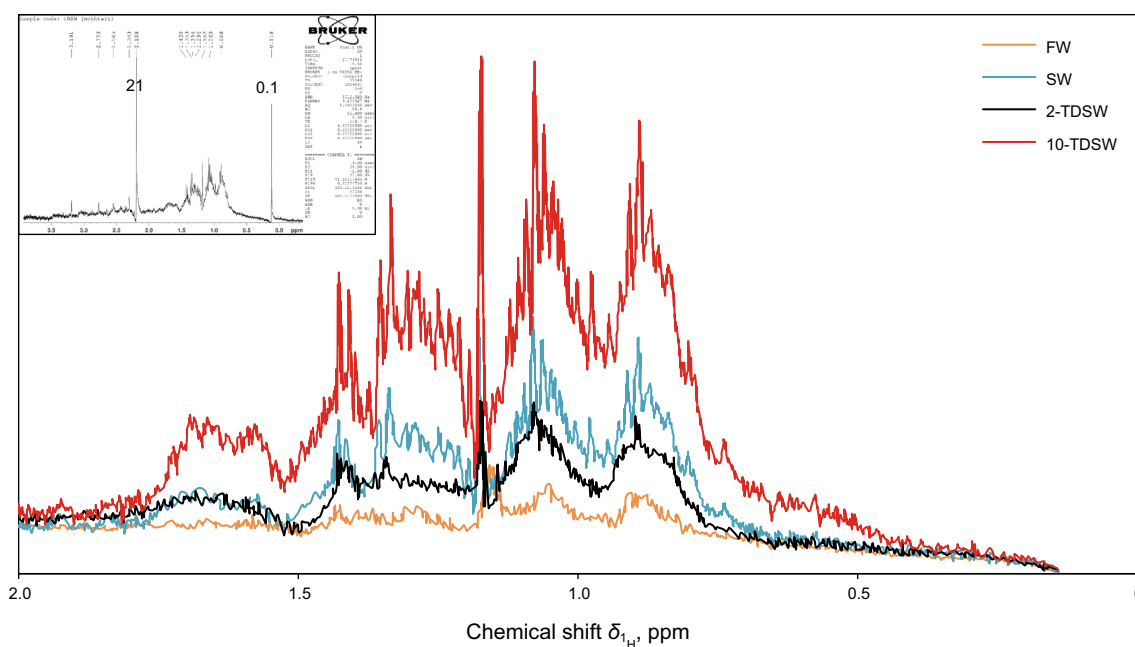
Fig. 6 NMR spectra of NAs dissociated in different brines after 45 days of being in contact with crude oil

components in the oil phase, brine salinity, brine pH and ions on emulsion stability (Abdel-Raouf 2012; Czarnecki et al. 2013; Dehghan et al. 2013; Fingas and Fieldhouse 2004; Kar et al. 2016; Maaref and Ayatollahi 2018; Mandal and Bera 2015; McLean and Kilpatrick 1997; Mohammed and Sorbie 2009, 2010; Mohammed et al. 1993; Moradi et al. 2010; Murray et al. 2009; Sullivan et al. 2007). Although the sweep efficiency of water flooding may increase through mobility control improvement from in situ oil-in-water emulsification (Mandal et al. 2010; McAuliffe 1973a, b; Moradi et al. 2014), the formation of water-in-oil emulsions increases the risk of trapping and unfavorable flow behavior of crude oil due to viscosity enhancement (Maaref et al. 2017; Rezaei and Firoozabadi 2014).
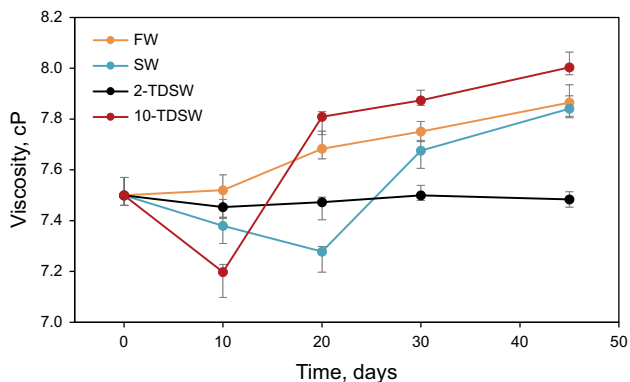

Fig. 8 The density of crude oil in contact with brines of different salinities over 45 days
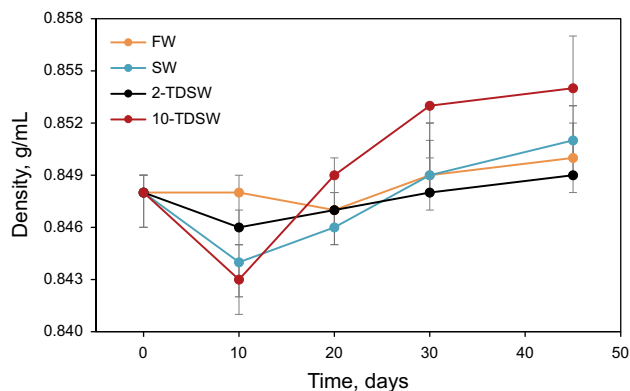

Fig. 7 The viscosity of crude oil in contact with brines of different salinities over 45 days
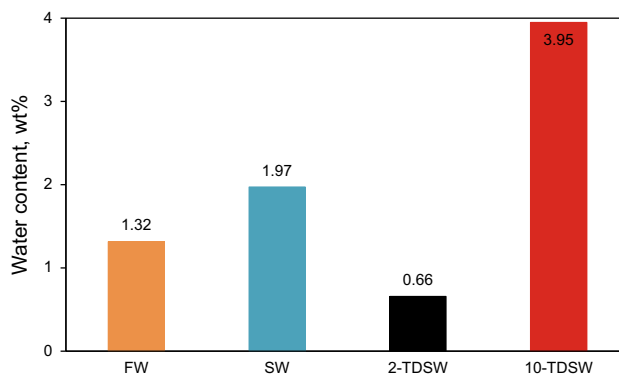

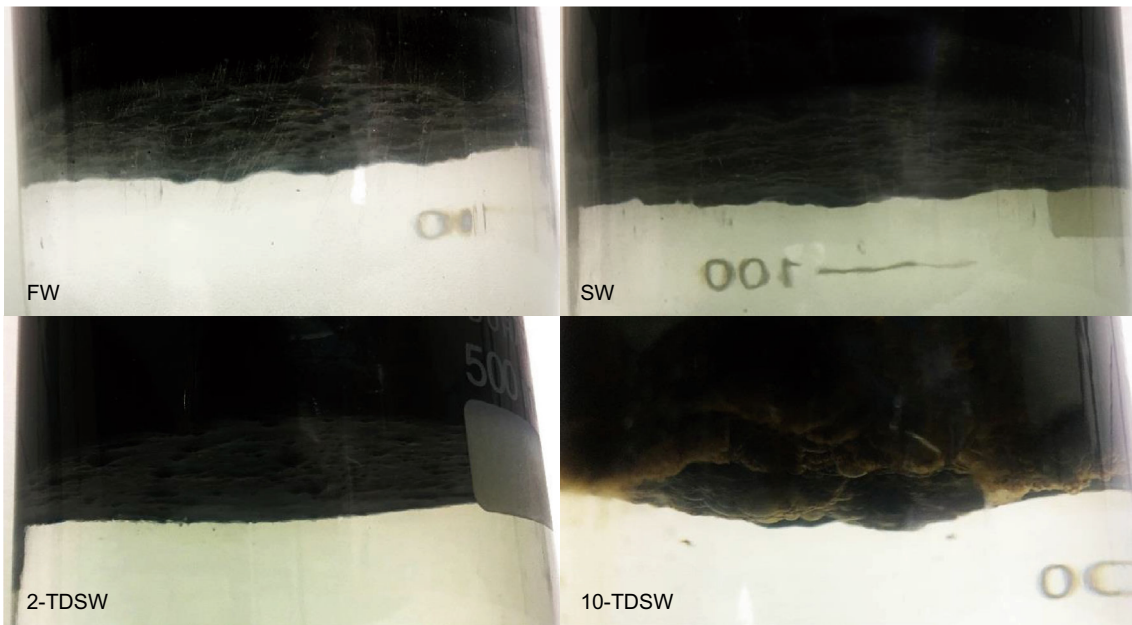**Fig. 9** Water content of oil samples in contact with different brines after 45 days

Fig. 10 Pictures for interface of crude oil–brine after 45 days of being in contact with different brines
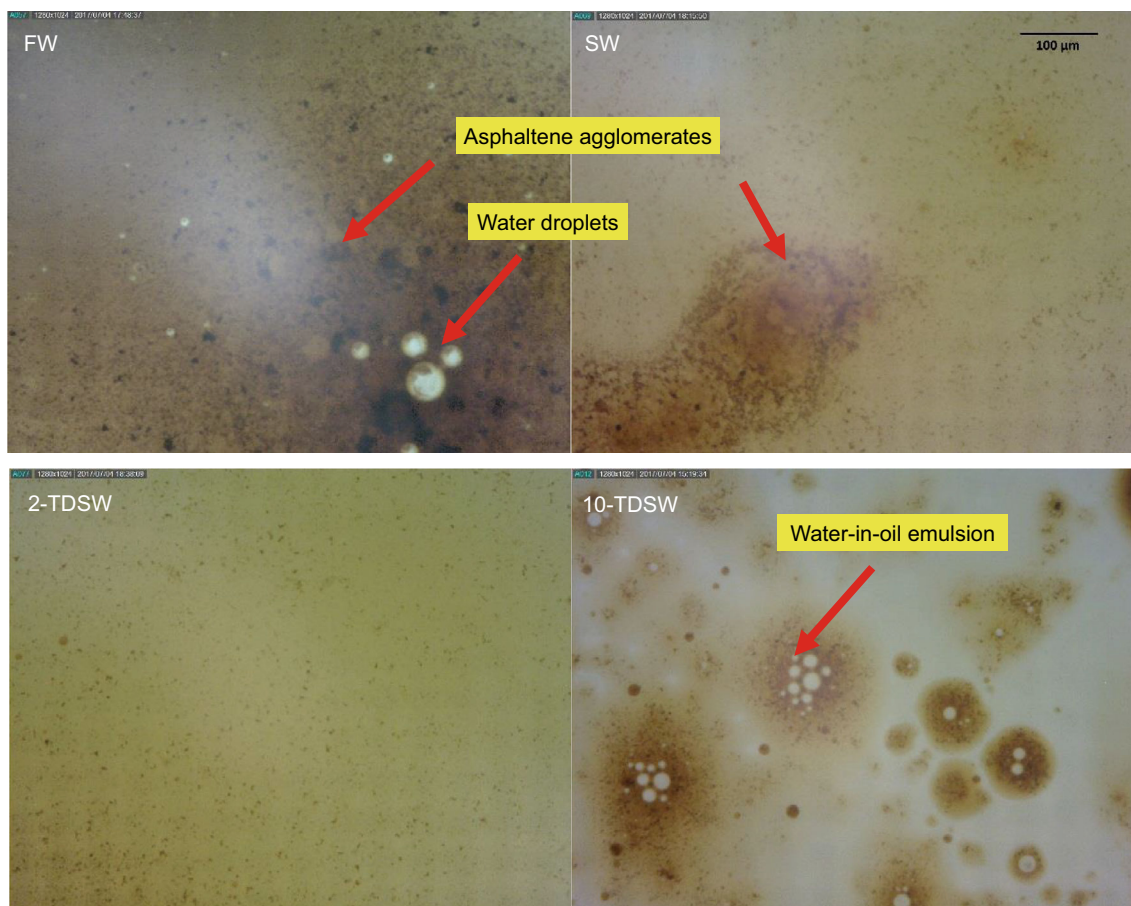

Fig. 11 Microscopic photographs for samples collected from interface of crude oil–brine at different salinities
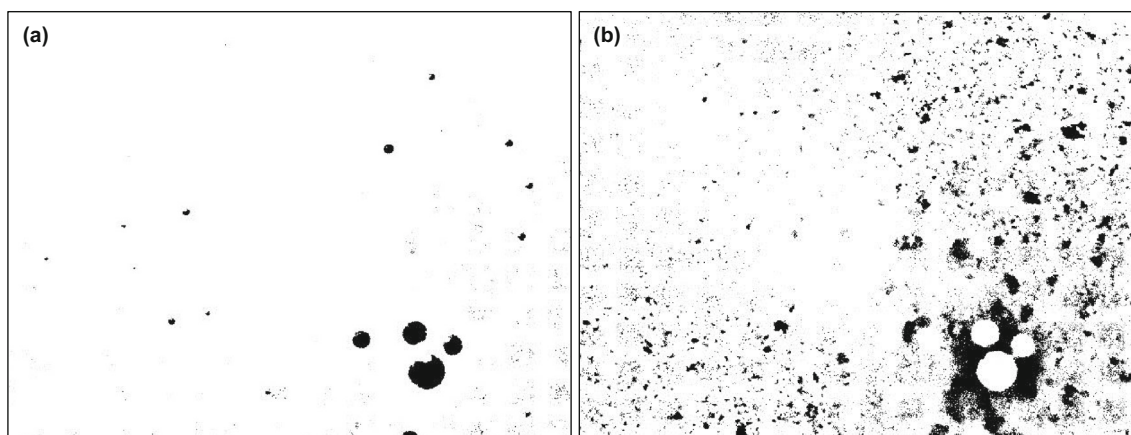
Fig. 12 Binary format of microscope photographs of FW to analyze water droplets (**a**) and asphaltene agglomerates (**b**)
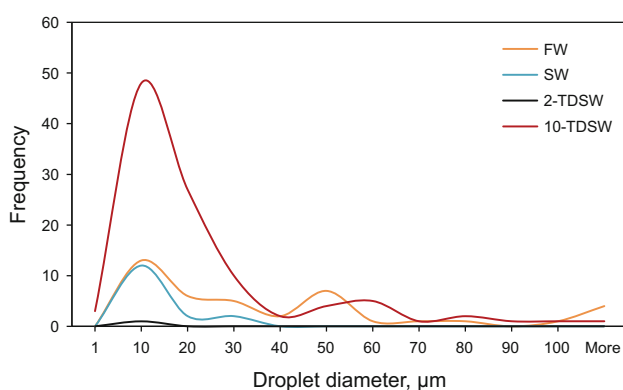

Fig. 13 Water droplet size distribution in water-in-oil emulsion created at the interface of crude oil–brine at different brines

Figure 7 clearly shows that the crude oil viscosity has remained approximately constant at 2-TDSW, while the crude oil samples in contact with brine of less and more salinities than 2-TDSW exhibit an increase in viscosity. The initial reduction in viscosity may illustrate the adsorption of high molecular weight fractions such as asphaltene molecules toward the interface and then the increase in viscosity is due to water-in-oil emulsion.

Another possible mechanism is the formation of insoluble complexes such as sodium and calcium naphthenates (NaN and CaN, respectively). Dissociated naphthenic acids may react with Na^+ or Ca^{2+} ions present in the brine, resulting in the formation of either soft-type emulsions due to NaN formation or hard solid-type deposits of CaN (Mohammed and Sorbie 2009, 2010). To investigate these hypotheses and to prove the emulsion formation which leads to viscosity increase, the density of samples was also measured. Figure 8 represents the density of crude oil samples in contact with different brines at different contact times.

The density alteration trends also confirm the results obtained from viscosity measurements. The initial reduction in density seems to be due to adsorption of asphaltene molecules toward the interface. This hypothesis needs more evidence to be proved. After that, an increase in crude oil density is observed because of water-in-oil emulsion. Relatively high oil density changes were observed for 10-TDSW which indicate the tendency for emulsification in this case. Figure 9 represents the water content of oil samples which was calculated from density data after 45 days. Obviously, the 10-TDSW and 2-TDSW samples show higher and lower water content, respectively.

Table 4 Results of image processing for samples collected from crude–brine interface

Brine	Total number of particles		Average size, µm		Volume fraction of particles	
	Water droplets	Asphaltene agglomerates	Water droplets	Asphaltene agglomerates	Water droplets	Asphaltene agglomerates
FW	41	4908	44.6	14.7	0.010275	0.092747
SW	16	1685	14.4	16.9	0.000218	0.03686
2-TDSW	1	1264	12.1	15.1	8.02E−06	0.019125
10-TDSW	105	1812	22.9	21.9	0.005845	0.091368

The condition of the interfaces after 45 days through visualization is also consistent with previous results. Figure 10 shows the pictures taken from interfaces of crude oil–brine after 45 days, which indicates the unstable interface and emulsion formation for 10-TDSW. The pH reduction due to the high amount of dissociated NAs for 10-TDSW, in addition to the adsorption of asphaltene molecules toward the interface because of the interface electrostatic attraction, leads to the profound effect on the interface condition.

To assess the results more accurately, a digital microscope was also used to monitor the interface condition, thoroughly. Figure 11 shows the microscopic pictures of samples which were collected from the interface.

Figure 10 clearly implies that the interface for 10-TDSW is far from sharp which indicates the ability to form a water-in-oil emulsion. However, the unstable interface for 10-TDSW indicates the emulsification, but the relatively sharp interface for other brines does not mean no emulsification. This is the reason for using digital microscopy to evaluate accurately the interface condition. Figure 11 shows that the interface for 2-TDSW is uniformly formed and has no aggregation; hence, no emulsification was observed. The result for the case of SW represents a transition state between two different cases of FW and 2-TDSW. The pictures also show that no water-in-oil emulsion is formed in SW.

For a deeper insight, a quantitative study of the microscopic pictures was conducted. The MATLAB image processing toolbox was utilized to analyze the pictures. Figure 12 represents the binary format of the microscopic images of FW which is used to measure the droplet size distribution, the mean size and the volume fraction of water droplets and the black clusters which may be asphaltene agglomerates. For more confidence about these black clusters, some of the samples were filtered through Whatman-42 filter paper and then washed with *n*-heptane. In all cases some black stains were observed on the surface of the filter paper which reveal that the black clusters in the figure are mostly asphaltene aggregates. The results are summarized in Fig. 13 and Table 4.

Figure 13 clearly indicates that the most common droplet size for all cases is about 10 μm; however, for the two cases of FW and 10-TDSW larger droplet sizes were also observed. As shown in Table 4, by reducing the salinity from FW to 2-TDSW, the number, mean size and volume fraction of water droplets decreased, while reducing the salinity beyond 2-TDSW leads to an increase in the number and volume fraction of water droplets. These results showed that at 2-TDSW both asphaltenes and NAs were adsorbed toward the interface, causing the formation of a stable interface and minimum changes in brine pH, crude oil viscosity and density. Obviously, water-in-oil emulsions

for both FW and 10-TDSW cases were observed; however, for FW the water droplets were fewer but larger than that for 10-TDSW. On the other hand, the asphaltene agglomerates for FW were more numerous but smaller than the ones for 10-TDSW. This finding is consistent with crude oil viscosity and density measurements previously presented in this section.
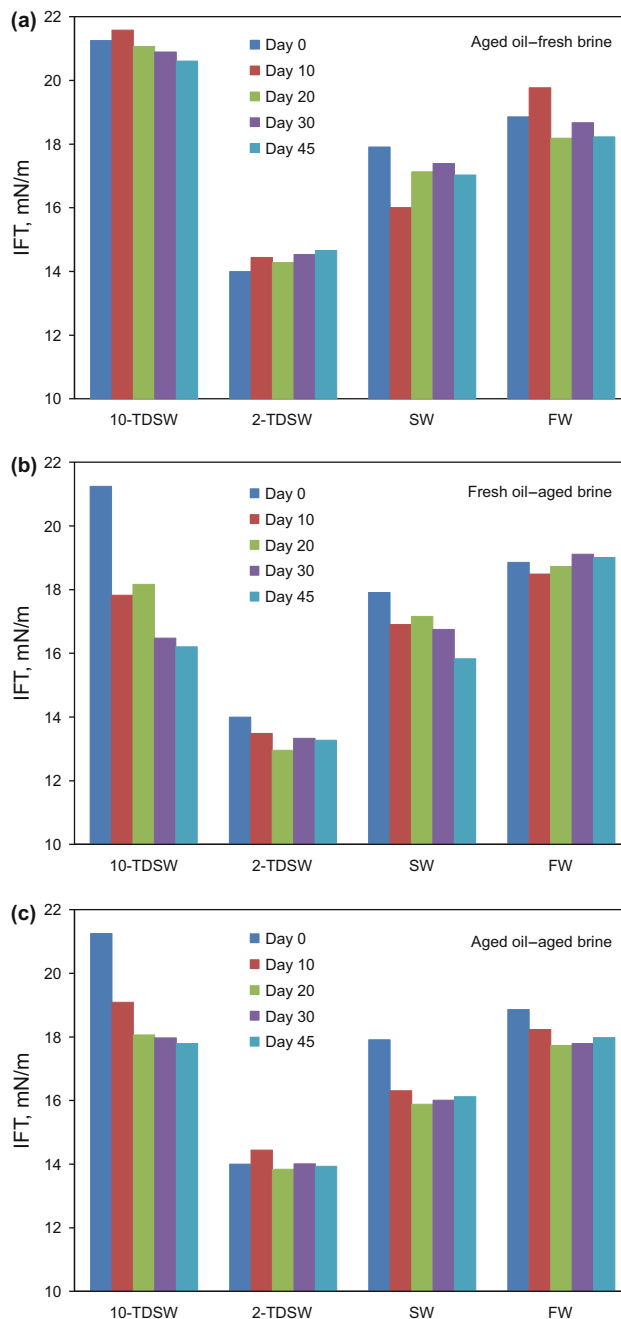

Fig. 14 IFT measurement for different brine salinities at three different experimental categories. **a** Aged oil–fresh brine. **b** Fresh oil–aged brine. **c** Aged oil–aged brine

3.5 IFT measurements

An overview of research papers on the IFT of crude oil–brine mixtures showed contradictory results (Abdel-Wali 1996; Bai et al. 2010; Cai et al. 1996; Dehghan et al. 2015a, b; Ikeda et al. 1992; Lashkarbolooki and Ayatollahi 2018; Mohamed et al. 1999; Serrano-Saldaña et al. 2004), as they report different IFT values, trends and governing mechanisms. In comparison with the pure systems, the IFT of crude oil–brine mixtures is complex functions of different parameters such as pressure, temperature, salinity, pH, TAN, and polar components which makes it more difficult to deal with (Buckley and Fan 2007). As described already in this research work, in order to have a clear understanding of the interactions between the aqueous phase and crude oil, three different types of IFT tests were designed as follow:

(1) fresh brine–aged crude oil, (2) aged brine–fresh crude oil and (3) aged brine–aged crude oil. Through these categories, separate outcomes of the tests for each phase were evaluated. Figure 14 shows the results of IFT tests separately for each experiment category. It is obvious that for all testing categories, 2-TDSW has the minimum IFT value. The salting-in effect and polarization of the interface due to ionic strength of the brine are the two main mechanisms which compete together on interfacial behavior. These processes result in the adsorption of asphaltene molecules on to the interface, dissociation of NAs in the aqueous solution, diffusion of surface active materials toward the interface and displacing, rearrangement and detachment of adsorbed polar components at the interface.

For 2-TDSW, the polarity of interface and length of the electrical double layer are sufficient for the adsorption of
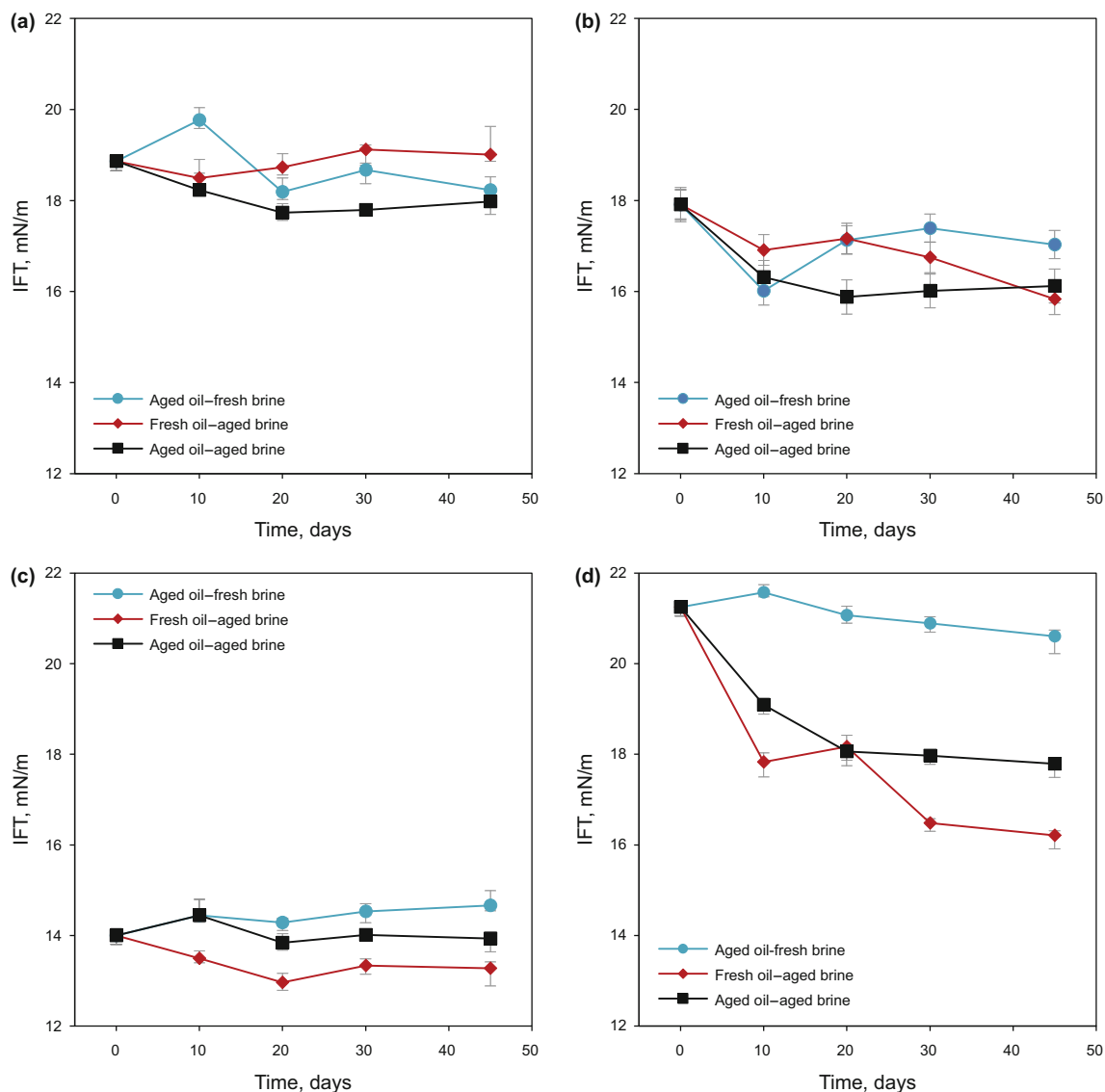

Fig. 15 IFT measurement at different contact times for FW–crude oil (**a**), SW–crude oil (**b**), 2-TDSW–crude oil (**c**) and 10-TDSW–crude oil (**d**)

both asphaltenes and NAs toward the interface to fill all empty sites; therefore, the accumulation of all polar components at the interface leads to lower interfacial tension, in comparison to the cases of brines with higher and lower salinities. However, since the detachment of surface active materials is negligible at this salinity, minimum changes in brine pH, crude oil viscosity and density were expected.

Figure 15 shows the IFT values for each brine–crude oil mixture by focusing on the effect of salinity on the measured values. Because of mass transfer between the two phases (brine and crude oil) in contact, their composition may alter, which affects the IFT values. Brine containing dissolved NAs (aged brine) has lower IFT with fresh crude oil compared to fresh brine. This indicates the effect of NAs in the solutions on the interface behavior. On the other hand, the IFT values of an aged crude oil, in which the polar components are decreased, in contact with fresh brine are greater than the ones for the fresh crude oil–fresh brine. Therefore, considering the IFT and the trends in three
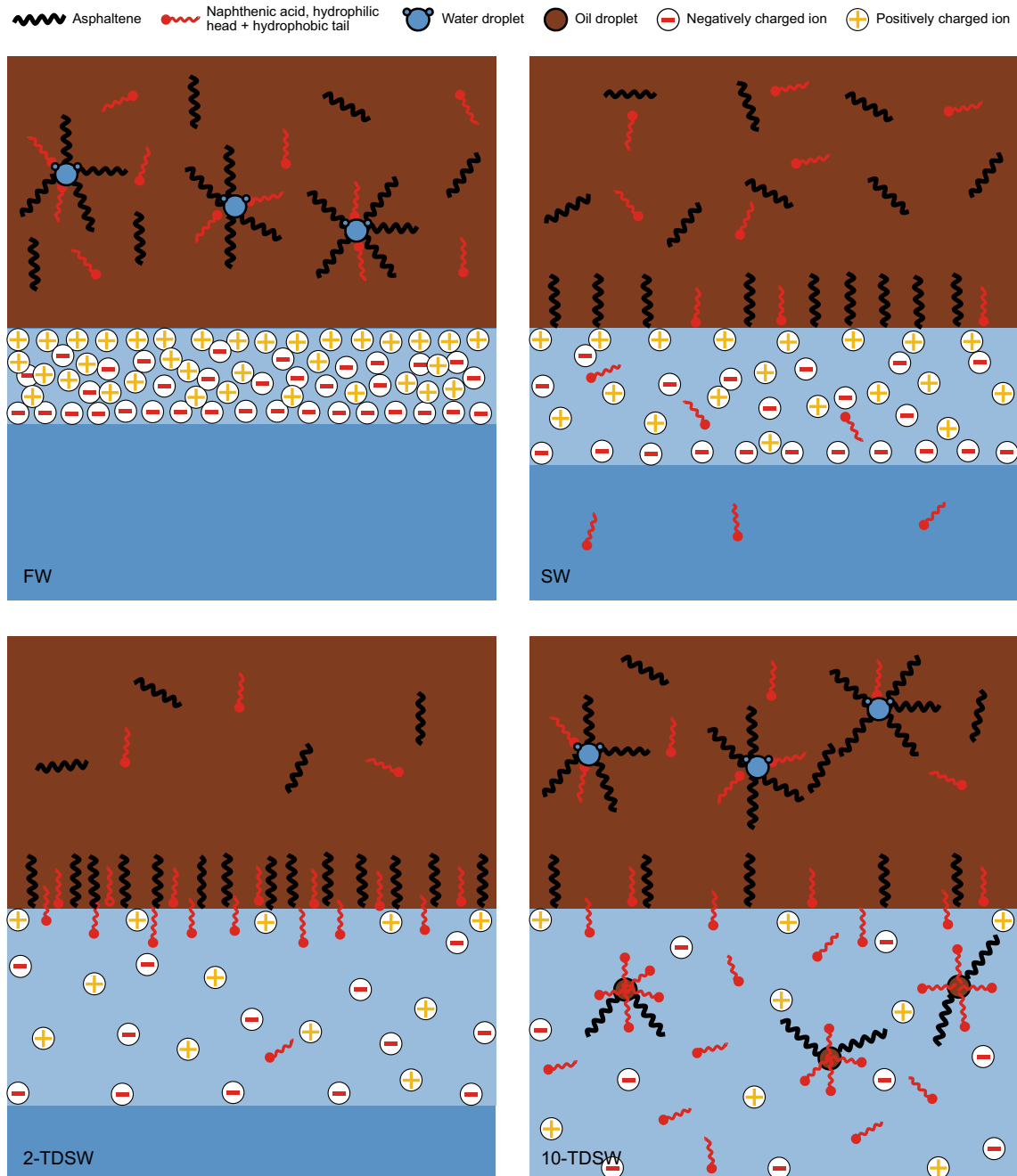

Fig. 16 Mechanisms of brine–crude oil interactions at different salinities

mentioned experiment categories can reveal the interactions between crude oil and the aqueous phase.

For high salinity water (FW), the Debye length is short and the brine has little tendency to dissolve the polar oil components. The accumulation of ions at the interface decreases the screening of the charge, reducing the adsorption of the polar components from the crude oil into the oil–brine interface. This is also supported by the results presented by other researchers that the high ionic strength of brine hinders the formation of the asphaltenic film (Moradi et al. 2013; Verruto et al. 2009). Hence, no significant changes in IFT values for all three categories are observed for the FW presented in Fig. 15a.

For SW, the rate of adsorption of asphaltenes to the interface is much higher than NAs (Moradi et al. 2013; Verruto et al. 2009). Therefore, asphaltene molecules in the crude oil move toward the interface competing with naphthenic components which hinders the transfer of NAs and affects its dissociation rate in brine (Moradi et al. 2013). In this salinity, asphaltenes adsorb onto the interface and NAs dissociate gently into the bulk brine. Because of this mechanism, the pH and conductivity of brine decline at very low rate. Since the amount of polar components in crude oil drops, the IFT values of the aged oil–fresh brine show an ascending trend, while IFT values for cases of fresh oil–aged brine and aged oil–aged brine display a descending trend, due to the presence of the transferred NAs inside the aged brine,.

When the salinity reduces, two opposing phenomena take place, salting-in and interface polarization. The competition between these two phenomena dictates the interaction response at the interface. At 2-TDSW, the ionic strength of the brine affects the adsorption of asphaltene molecules at the interface due to the polarization of the interface. Moreover, other surface active materials diffuse toward the interface to occupy the surface sites. The accumulation of all surface active agents at the interface leads to lower IFT values compared to the cases of brines with other salinities. On the other hand, for 2-TDSW less changes are observed in brine pH, crude oil viscosity and density which confirms this hypothesis. Therefore, the low IFT values remain unchanged for all three cases observed in Fig. 15c for 2SW.

At lower salinities, such as 10-TDSW, the salting-in effect dominates the interface polarization effect. The competition between different polar components to adsorb at the interface can affect the arrangement of surface active materials and the availability of the empty sites at the interface. Besides, the primarily adsorbed polar components may detach from the interface. During the detachment of NAs and asphaltenes from the interface, water-in-oil emulsions are formed. Consequently, the pH of the aqueous phase drops drastically and the crude oil viscosity
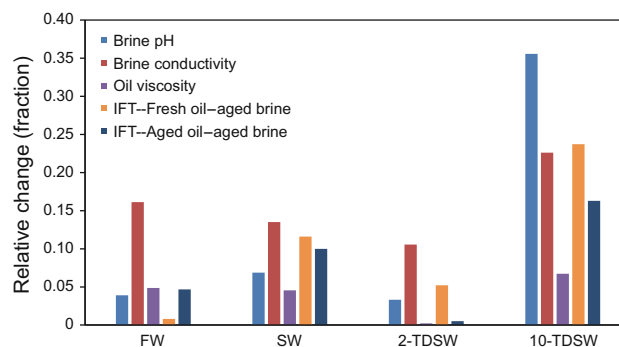
Fig. 17 Relative changes of different brine and crude oil properties after 45 days of contact

and density increase. Because of the acidity of aged water and high concentration of NAs, IFT trends for both cases of fresh oil–aged brine and aged oil–aged brine are sharply descending (see Fig. 15d). Similarly, due to the detachment of asphaltenes from the interface, IFT values at this salinity exhibit a slight reduction for aged oil–fresh brine cases. All proposed mechanisms are summarized in Fig. 16.

To examine the validity of the aforementioned discussion, relative changes of the mentioned physical properties were calculated and compared with each other as shown in Fig. 17. The results show the consistency of the findings in this research work and verify the proposed mechanisms. When partitioning of crude oil polar components increased, the rate of change of all the measured properties, brine pH, brine conductivity, crude oil viscosity and density and IFT increased. Figure 17 indicates that crude oil and brine properties experience critical changes during low salinity water flooding. For example, in the case of 10-TDSW, which is shown to have the highest relative change for all parameters, the brine pH, brine conductivity, oil viscosity and interfacial tension were changed by 35%, 22%, 6% and 16%, respectively. These changes may affect the multiphase fluids flow, governing mechanisms for wettability alteration, production mechanisms and finally the oil recovery efficiency of low salinity water flooding. It is important to note that all experiments conducted in this study were performed at static conditions; hence, the mass transfer is diffusion controlled. The shear between the crude oil and the brine when they flow in the porous rock may result in much larger physical property changes and may improve the conditions for better recovery.

4 Conclusions

This research work is based on the fact that the physical properties of brine and crude oil are altered when they are preserved in contact for a period of time. This critically affects the performance of the low salinity water flooding

in oil reservoirs. Although the results seem to be limited to the current crude oil sample, considering its different parameters such as acid/base number and asphaltene content that affect the rate and intensity of the interactions, the mechanisms and concepts behind the phenomena as follows are remained unchanged.

1. The interfacial behavior during the preservation of the crude oil in contact with brine is the result of several synergistic and opposing interfacial phenomena. Those include salting-in and salting-out effects, polarization of the crude oil–brine interface due to ionic strength of the brine and dissociation of the polar components such as NAs in the brine. Besides, the adsorption of asphaltene molecules onto the interface, diffusion of the surface active materials through the crude oil or brine toward the interface, and rearrangement, detachment and movement of the adsorbed components at the interface influence this behavior.

2. Ionic strength considerably affects the kinetics of adsorption of asphaltene onto the interface and partitioning of the NAs in the aqueous phase. In general, as the ionic strength of brine decreases, the partitioning and dissociation of NAs increase. Therefore, physical properties of both crude oil and brine change more compared to the higher ionic strength solutions.

3. There is an ionic strength in which the relative changes of physical properties are negligible and the lowest IFT is observed.

4. The results indicate relatively considerable changes in oil viscosity, density and interfacial tension between crude oil and the 10 times diluted seawater during the mentioned contact time. In conclusion, these changes may significantly modify the sweep efficiency after a long period of time in the reservoir during low salinity water flooding.

5. In agreement with other experimental results, UV–Vis and ^{1}H NMR spectroscopy show higher peak intensity for the 10 times diluted seawater compared to others, which indicates the presence of higher amounts of NAs in 10 times diluted seawater.

6. Considering the crude oil viscosity alteration, oil density results and the visual study of the tests, the formation of water-in-oil emulsions for the 10 times diluted seawater is confirmed.

7. The dissociation of NAs in the brine which drastically reduces pH has the potential to alter the wettability of the rock toward more water wet state. This hypothesis will be investigated in future work.

References

Abdel-Raouf ME-S. Factors affecting the stability of crude oil emulsions. In: Crude oil emulsions: composition stability and characterization. Abdel-Raouf ME-S. Editor. InTech; 2012. Available from: http://www.intechopen.com/books/crude-oil-emulsions-compositionstability-and-characterization/factors-affecting-the-stability-of-crude-oil-emulsions.

Abdel-Wali AA. Effect of simple polar compounds and salinity on interfacial tension and wettability of rock/oil/brine system effect. J King Saud Univ. 1996;8:153–63.

Al-Attar HH, Mahmoud MY, Zekri AY, Almehaideb RA, Ghannam MT. The impact of LoSal on oil recovery from a selected carbonate reservoir in Abu Dhabi—an experimental approach. In: SPE middle east oil gas show conference, March, Manama, Bahrain; 2013. https://doi.org/10.2118/164331-MS.

Al-Shalabi EW, Sepehrnoori K. A comprehensive review of low salinity/engineered water injections and their applications in sandstone and carbonate rocks. J Pet Sci Eng. 2016;139:137–61. https://doi.org/10.1016/j.petrol.2015.11.027.

Alvarado V, Wang X, Moradi M. Role of acid components and asphaltenes in Wyoming water-in-crude oil emulsions. Energy Fuels. 2011;25(10):4606–13. https://doi.org/10.1021/ef2010805.

Austad T. Water-based EOR in carbonates and sandstones: new chemical understanding of the EOR potential using "smart water". In: Enhanced oil recovery: field case studies. Sheng J. Editor. Oxford: Elsevier; 2013, p. 301–35.

Austad T, Shariatpanahi SF, Strand S, Black CJJ, Webb KJ. Conditions for a low-salinity enhanced oil recovery (EOR) effect in carbonate oil reservoirs. Energy Fuels. 2011;26(1):569–75. https://doi.org/10.1021/ef201435g.

Badertscher M, Bühlmann P, Pretsch E. Structure determination of organic compounds. Berlin: Springer; 2009.

Bai J-M, Fan W-Y, Nan G-Z, Li S-P, Yu B-S. Influence of interaction between heavy oil components and petroleum sulfonate on the oil–water interfacial tension. J Dispers Sci Technol. 2010;31(4):551–6. https://doi.org/10.1080/01932690903167475.

Buckley JS, Fan T. Crude oil/brine interfacial tensions 1. Petrophysics. 2007;48(3):175–85.

Cai B-Y, Yang J-T, Guo T-M. Interfacial tension of hydrocarbon + water/brine systems under high pressure. J Chem Eng Data. 1996;41(3):493–6. https://doi.org/10.1021/je950259a.

Cratin PD. Mathematical modeling of some pH-dependent surface and interfacial properties of stearic acid. J Dispers Sci Technol. 1993;14(5):559–602. https://doi.org/10.1080/01932699308943427.

Czarnecki J, Tchoukov P, Dabros T, Xu Z. Role of asphaltenes in stabilisation of water in crude oil emulsions. Can J Chem Eng. 2013;91(8):1365–71. https://doi.org/10.1002/cjce.21835.

Dehghan AA, Masihi M, Ayatollahi S. Evaluation of chemicals interaction with heavy crude oil through water/oil emulsion and interfacial tension study. Energy Fuels. 2013;27(10):5852–60. https://doi.org/10.1021/ef401361t.

Dehghan AA, Masihi M, Ayatollahi S. Phase behavior and interfacial tension evaluation of a newly designed surfactant on heavy oil displacement efficiency; effects of salinity, wettability, and capillary pressure. Fluid Phase Equilib. 2015a;396:20–7. https://doi.org/10.1016/j.fluid.2015.03.028.

Dehghan AA, Masihi M, Ayatollahi S. Interfacial tension and wettability change phenomena during alkali–surfactant interactions with acidic heavy crude oil. Energy Fuels. 2015b;29(2):649–58. https://doi.org/10.1021/ef502435y.

Drelich J, Fang C, White CL. Measurement of interfacial tension in fluid–fluid systems. Encycl Surf Colloid Sci. 2002;3:3158–63.

Emadi A, Sohrabi M. Visual investigation of oil recovery by low salinity water injection: formation of water micro-dispersions and wettability alteration. In: SPE annual technical conference and exhibition, 30 September–2 October, New Orleans, Louisiana, USA; 2013. https://doi.org/10.2118/166435-MS.

Fingas M, Fieldhouse B. Formation of water-in-oil emulsions and application to oil spill modelling. J Hazard Mater. 2004;107(1):37–50. https://doi.org/10.1016/j.jhazmat.2003.11.008.

Garcia-Olvera G, Reilly TM, Lehmann TE, Alvarado V. Effects of asphaltenes and organic acids on crude oil–brine interfacial visco-elasticity and oil recovery in low-salinity waterflooding. Fuel. 2016;185:151–63. https://doi.org/10.1016/j.fuel.2016.07.104.

Guo J, Cao J, Li M, Xia H. Influences of water treatment agents on oil-water interfacial properties of oilfield produced water. Pet Sci. 2013;10(3):415–20. https://doi.org/10.1007/s12182-013-0290-5.

Gupta R, Mohanty KK. Wettability alteration mechanism for oil recovery from fractured carbonate rocks. Transp Porous Media. 2011;87(2):635–52. https://doi.org/10.1007/s11242-010-9706-5.

Hamam SEM, Hamoda MF, Shaban HI, Kilani AS. Crude oil dissolution in saline water. Water Air Soil Pollut. 1988;37(1):55–64. https://doi.org/10.1007/BF00226479.

Hiemenz PC, Rajagopalan R. Principles of colloid and surface chemistry, revised and expanded. Boca Raton: CRC Press; 1997.

Ikeda N, Aratono M, Motomura K. Thermodynamic study on the adsorption of sodium chloride at the water/hexane interface. J Colloid Interface Sci. 1992;149(1):208–15. https://doi.org/10.1016/0021-9797(92)90405-B.

Kar S, Kakati H, Mandal A, Laik S. Experimental and modeling study of kinetics for methane hydrate formation in a crude oil-in-water emulsion. Pet Sci. 2016;13(3):489–95. https://doi.org/10.1007/s12182-016-0108-3.

Karimi M, Al-Maamari RS, Ayatollahi S, Mehranbod N. Wettability alteration and oil recovery by spontaneous imbibition of low salinity brine into carbonates: impact of Mg^{2+}, SO_4^{2-} and cationic surfactant. J Pet Sci Eng. 2016;147:560–9. https://doi.org/10.1016/j.petrol.2016.09.015.

Kazemi Nia Korrani A. Mechanistic modeling of low salinity water injection. 2014. https://repositories.lib.utexas.edu/handle/2152/28472.

Lashkarbolooki M, Ayatollahi S. Effect of asphaltene and resin on interfacial tension of acidic crude oil/sulfate aqueous solution: experimental study. Fluid Phase Equilib. 2016;414:149–55. https://doi.org/10.1016/j.fluid.2016.01.032.

Lashkarbolooki M, Ayatollahi S. Evaluation of effect of temperature and pressure on the dynamic interfacial tension of crude oil/aqueous solutions containing chloride anion through experimental and modelling approaches. Can J Chem Eng. 2018;96(6):1396–402. https://doi.org/10.1002/cjce.23059.

Lashkarbolooki M, Ayatollahi S, Riazi M. The impacts of aqueous ions on interfacial tension and wettability of an asphaltenic-acidic crude oil reservoir during smart water injection. J Chem

Eng Data. 2014a;59(11):3624–34. https://doi.org/10.1021/je500730e.

Lashkarbolooki M, Ayatollahi S, Riazi M. Effect of salinity, resin, and asphaltene on the surface properties of acidic crude oil/smart water/rock system. Energy Fuels. 2014b;28(11):6820–9. https://doi.org/10.1021/ef5015692.

Lashkarbolooki M, Ayatollahi S, Riazi M. Mechanistic study on the dynamic interfacial tension of crude oil + water systems: experimental and modeling approaches. J Ind Eng Chem. 2016a;35:408–16. https://doi.org/10.1016/j.jiec.2016.01.025.

Lashkarbolooki M, Riazi M, Ayatollahi S, Hezave AZ. Synergy effects of ions, resin, and asphaltene on interfacial tension of acidic crude oil and low–high salinity brines. Fuel. 2016b;165:75–85. https://doi.org/10.1016/j.fuel.2015.10.030.

Lashkarbolooki M, Riazi M, Hajibagheri F, Ayatollahi S. Low salinity injection into asphaltenic-carbonate oil reservoir, mechanistical study. J Mol Liq. 2016c;216:377–86. https://doi.org/10.1016/j.molliq.2016.01.051.

Li Y. Oil recovery by low salinity water injection into a reservoir: a new study of tertiary oil recovery mechanism. Transp Porous Media. 2011;90(2):333–62. https://doi.org/10.1007/s11242-011-9788-8.

Maaref S, Ayatollahi S. The effect of brine salinity on water-in-oil emulsion stability through droplet size distribution analysis: a case study. J Dispers Sci Technol. 2018;39(5):721–33. https://doi.org/10.1080/01932691.2017.1386569.

Maaref S, Ayatollahi S, Rezaei N, Masihi M. The effect of dispersed phase salinity on water-in-oil emulsion flow performance: a micromodel study. Ind Eng Chem Res. 2017;56(15):4549–61. https://doi.org/10.1021/acs.iecr.7b00432.

Mandal A, Bera A. Modeling of flow of oil-in-water emulsions through porous media. Pet Sci. 2015;12(2):273–81. https://doi.org/10.1007/s12182-015-0025-x.

Mandal A, Samanta A, Bera A, Ojha K. Characterization of oil–water emulsion and its use in enhanced oil recovery. Ind Eng Chem Res. 2010;49(24):12756–61. https://doi.org/10.1021/ie101589x.

McAuliffe CD. Crude-oil-water emulsions to improve fluid flow in an oil reservoir. J Pet Technol. 1973a;25(6):721–6. https://doi.org/10.2118/4370-PA.

McAuliffe CD. Oil-in-water emulsions and their flow properties in porous media. J Pet Technol. 1973b;25(6):727–33. https://doi.org/10.2118/4369-PA.

McLean JD, Kilpatrick PK. Effects of asphaltene solvency on stability of water-in-crude-oil emulsions. J Colloid Interface Sci. 1997;189(2):242–53. https://doi.org/10.1006/jcis.1997.4807.

McPhee C, Reed J, Zubizarreta I. Core analysis: a best practice guide. New York: Elsevier; 2015.

Mohamed RS, Ramos ACS, Loh W. Aggregation behavior of two asphaltenic fractions in aromatic solvents. Energy Fuels. 1999;13(2):323–7. https://doi.org/10.1021/ef9802072.

Mohammed MA, Sorbie KS. Naphthenic acid extraction and characterization from naphthenate field deposits and crude oils using ESMS and APCI-MS. Colloids Surf A Physicochem Eng Asp. 2009;349(1–3):1–18. https://doi.org/10.1016/j.colsurfa.2009.07.047.

Mohammed MA, Sorbie KS. Thermodynamic modelling of calcium naphthenate formation: model predictions and experimental results. Colloids Surf A Physicochem Eng Asp. 2010;369(1–3):1–10. https://doi.org/10.1016/j.colsurfa.2010.08.034.

Mohammed RA, Bailey AI, Luckham PF, Taylor SE. Dewatering of crude oil emulsions. 2. Interfacial properties of the asphaltic constituents of crude oil. Colloids Surf A Physicochem Eng Asp. 1993;80(2–3):237–42. https://doi.org/10.1016/0927-7757(93)80203-Q.

Mohanty KK, Chandrasekhar S. Wettability alteration with brine composition in high temperature carbonate reservoirs. In: SPE annual technical conference and exhibition, 30 September–2 October, New Orleans, Louisiana, USA; 2013. https://doi.org/10.2118/166280-MS.

Moradi M, Alvarado V, Huzurbazar S. Effect of salinity on water-in-crude oil emulsion: evaluation through drop-size distribution proxy. Energy Fuels. 2010;25(1):260–8. https://doi.org/10.1021/ef101236h.

Moradi M, Topchiy E, Lehmann TE, Alvarado V. Impact of ionic strength on partitioning of naphthenic acids in water–crude oil systems—determination through high-field NMR spectroscopy. Fuel. 2013;112:236–48. https://doi.org/10.1016/j.fuel.2013.05.024.

Moradi M, Kazempour M, French JT, Alvarado V. Dynamic flow response of crude oil-in-water emulsion during flow through porous media. Fuel. 2014;135:38–45. https://doi.org/10.1016/j.fuel.2014.06.025.

Morrow N, Buckley J. Improved oil recovery by low-salinity waterflooding. J Pet Technol. 2011;63(5):106–12. https://doi.org/10.2118/129421-JPT.

Murray BS, Dickinson E, Wang Y. Bubble stability in the presence of oil-in-water emulsion droplets: influence of surface shear versus dilatational rheology. Food Hydrocoll. 2009;23(4):1198–208. https://doi.org/10.1016/j.foodhyd.2008.07.015.

Nasralla RA, Alotaibi MB, Nasr-El-Din HA. Efficiency of oil recovery by low salinity water flooding in sandstone reservoirs. In: SPE Western North American region meeting, 7–11 May, Anchorage, Alaska, USA; 2011. https://doi.org/10.2118/144602-MS.

Peters F, Arabali D. Interfacial tension between oil and water measured with a modified contour method. Colloids Surf A Physicochem Eng Asp. 2013;426:1–5. https://doi.org/10.1016/j.colsurfa.2013.03.010.

Rezaei N, Firoozabadi A. Macro-and microscale waterflooding performances of crudes which form w/o emulsions upon mixing with brines. Energy Fuels. 2014;28(3):2092–103. https://doi.org/10.1021/ef402223d.

RezaeiDoust A, Puntervold T, Strand S, Austad T. Smart water as wettability modifier in carbonate and sandstone: a discussion of similarities/differences in the chemical mechanisms. Energy Fuels. 2009;23(9):4479–85. https://doi.org/10.1021/ef900185q.

Schobert H. Chemistry of fossil fuels and biofuels. Cambridge: Cambridge University Press; 2013.

Seccombe JC, Lager A, Webb KJ, Jerauld G, Fueg E. Improving waterflood recovery: LoSalTM EOR field evaluation. In: SPE symposium on improved oil recovery, 20–23 April, Tulsa, Oklahoma, USA; 2008. https://doi.org/10.2118/113480-MS.

Seifert WK, Howells WG. Interfacially active acids in a California crude oil. Isolation of carboxylic acids and phenols. Anal Chem. 1969;41(4):554–62. https://doi.org/10.1021/ac60273a002.

Serrano-Saldaña E, Domínguez-Ortiz A, Pérez-Aguilar H, Kornhauser-Strauss I, Rojas-González F. Wettability of solid/brine/n-dodecane systems: experimental study of the effects of ionic strength and surfactant concentration. Colloids Surfaces A Physicochem Eng Asp. 2004;241(1):343–9. https://doi.org/10.1016/j.colsurfa.2004.04.025.

Speight JG. The chemistry and technology of petroleum. Boca Raton: CRC Press; 2014.

Strand S, Høgnesen EJ, Austad T. Wettability alteration of carbonates—effects of potential determining ions (Ca^{2+} and SO_4^{2-}) and temperature. Colloids Surfaces A Physicochem Eng Asp. 2006;275(1–3):1–10. https://doi.org/10.1016/j.colsurfa.2005.10.061.

Sullivan AP, Zaki NN, Sjöblom J, Kilpatrick PK. The stability of water-in-crude and model oil emulsions. Can J Chem Eng. 2007;85(6):793–807. https://doi.org/10.1002/cjce.5450850601.

Tang GQ, Morrow NR. Salinity, temperature, oil composition, and oil recovery by waterflooding. SPE Reserv Eng. 1997;12(4):269–76. https://doi.org/10.2118/36680-PA.

Tang GQ, Morrow NR. Influence of brine composition and fines migration on crude/oil/rock interactions and oil recovery. J Pet Sci Eng. 1999;24:99–111. https://doi.org/10.1016/S0920-4105(99)00034-0.

Verruto VJ, Le RK, Kilpatrick PK. Adsorption and molecular rearrangement of amphoteric species at oil–water interfaces. J Phys Chem B. 2009;113(42):13788–99. https://doi.org/10.1021/jp902923j.

Yarranton HW, Masliyah JH. Gibbs–Langmuir model for interfacial tension of nonideal organic mixtures over water. J Phys Chem. 1996;100(5):1786–92. https://doi.org/10.1021/jp952017n.

Yildiz HO, Morrow NR. Effect of brine composition on recovery of Moutray crude oil by waterflooding. J Pet Sci Eng. 1996;14:159–68. https://doi.org/10.1016/0920-4105(95)00041-0.

Yousef AA, Al-Saleh S, Al-Kaabi AU, Al-Jawfi MS. Laboratory investigation of novel oil recovery method for carbonate reservoirs. In: Canadian unconventional resources and international petroleum conference SPE-137634-MS. Calgary, Alberta, Canada; 2010. https://doi.org/10.2118/137634-MS.

Zaeri MR, Hashemi R, Shahverdi H, Sadeghi M. Enhanced oil recovery from carbonate reservoirs by spontaneous imbibition of low salinity water. Pet Sci. 2018;12:122. https://doi.org/10.1007/s12182-018-0234-1.